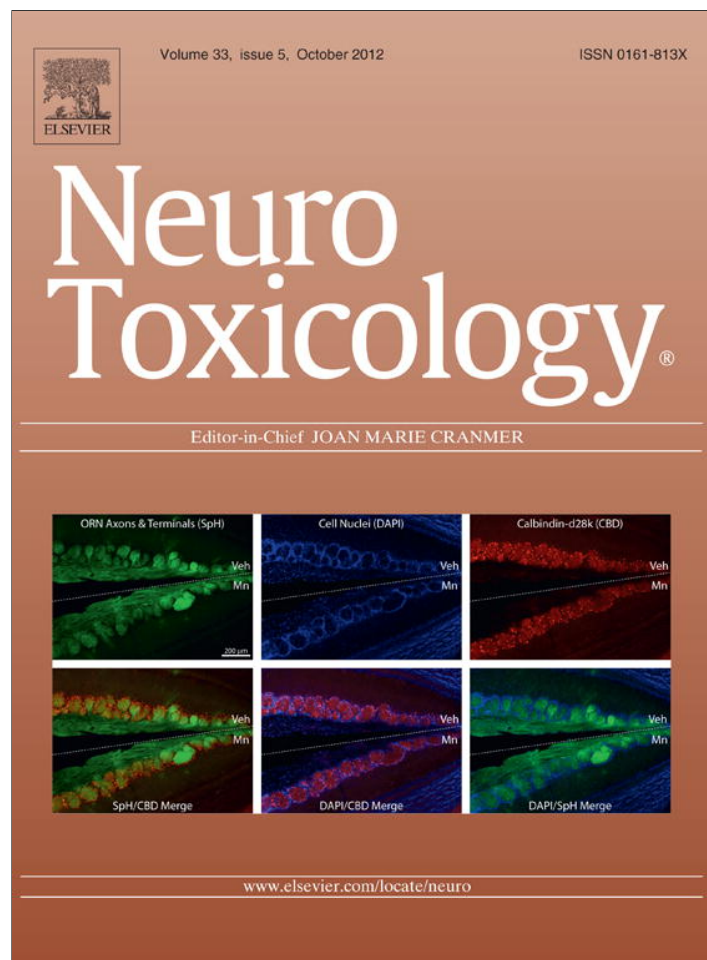


Provided for non-commercial research and education use.
Not for reproduction, distribution or commercial use.



This article appeared in a journal published by Elsevier. The attached copy is furnished to the author for internal non-commercial research and education use, including for instruction at the authors institution and sharing with colleagues.

Other uses, including reproduction and distribution, or selling or licensing copies, or posting to personal, institutional or third party websites are prohibited.

In most cases authors are permitted to post their version of the article (e.g. in Word or Tex form) to their personal website or institutional repository. Authors requiring further information regarding Elsevier's archiving and manuscript policies are encouraged to visit:

<http://www.elsevier.com/copyright>



Neurite outgrowth and differentiation of rat cortex progenitor cells are sensitive to lithium chloride at non-cytotoxic exposures[☆]

Kavita M. Jeerage^{*}, Tammy L. Oreskovic, Stephanie L. Hume

Materials Reliability Division, National Institute of Standards and Technology, 325 Broadway, Boulder, CO 80305, USA

ARTICLE INFO

Article history:

Received 17 October 2011

Accepted 25 June 2012

Available online 4 July 2012

Keywords:

Neurite outgrowth

Progenitor cells

Lithium chloride

ABSTRACT

Neuron-specific *in vitro* screening strategies have the potential to accelerate the evaluation of chemicals for neurotoxicity. We examined neurite outgrowth as a measure of neuronal response with a commercially available rat cortex progenitor cell model, where cells were exposed to a chemical during a period of cell differentiation. In control cultures, the fraction of beta-III-tubulin positive neurons and their neurite length increased significantly with time, indicating differentiation of the progenitor cells. Expression of glial fibrillary acidic protein, an astrocyte marker, also increased significantly with time. By seeding progenitor cells at varying densities, we demonstrated that neurite length was influenced by cell–cell spacing. After ten days, cultures seeded at densities of 1000 cells/mm² or lower had significantly shorter neurites than cultures seeded at densities of 1250 cells/mm² or higher. Progenitor cells were exposed to lithium, a neuroactive chemical with diverse modes of action. Cultures exposed to 30 mmol/L or 10 mmol/L lithium chloride (LiCl) had significantly lower metabolic activity than control cultures, as reported by adenosine triphosphate content, and no neurons were observed after ten days of exposure. Cultures exposed to 3 mmol/L, 1 mmol/L, or 0.3 mmol/L LiCl, which encompass lithium's therapeutic range, had metabolic activity similar to control cultures. These cultures exhibited concentration-dependent decreases in neurite outgrowth after ten days of LiCl exposure. Neurite outgrowth results were relatively robust, regardless of the evaluation methodology. This work demonstrates that measurement of neurite outgrowth in differentiating progenitor cell cultures can be a sensitive endpoint for neuronal response under non-cytotoxic exposure conditions.

Published by Elsevier Inc.

1. Introduction

Early exposure to neurotoxic compounds may lead to developmental disorders and subclinical loss of function due to the vulnerability of the developing brain (Grandjean and Landrigan, 2006). Within the cerebral cortex, specific disruptions to neurogenesis, migration, differentiation, dendrite formation, and synaptogenesis lead to long-term anatomical, neurochemical, and/or behavioral abnormalities in rodents (Berger-Sweeney and Hohmann, 1997). In humans, development continues for years after birth (Rodier, 1995), making developmental neurotoxicity an important component of toxicity evaluations. Although it is recognized that neurotoxins are likely to damage the developing brain at lower doses than those which affect adults (Tilson, 2000), most chemicals have not been evaluated for developmental neurotoxicity (Goldman and Koduru, 2000). *In vivo* methods

accepted by the U.S. Environmental Protection Agency or the Organization for Economic Cooperation and Development are expensive, time-intensive, and not suitable for screening large numbers of chemicals (Radio and Mundy, 2008). Rapid and inexpensive *in vitro* experiments utilizing cell lines, primary cells, or explants have often been designed to examine specific hypotheses (Harry et al., 1998). Although it appears unlikely that *in vitro* methods could completely replace animal studies, validated assays could be applied in a tiered screening strategy to identify neurotoxic hazards (Crofton et al., 2011; Lein et al., 2007). A key requirement is endpoints that are specific to neural cells, in addition to biochemical endpoints common to all mammalian cells (Bal-Price et al., 2010; Harry and Tiffany-Castiglioni, 2005).

One promising strategy for *in vitro* screening involves assaying key neurodevelopmental processes such as proliferation, migration, differentiation, axonal and dendritic outgrowth, and synaptogenesis. Despite probable diverse mechanisms, developmental neurotoxins are expected to disrupt these vulnerable cellular processes, which are highly conserved across species (Barone et al., 2000; Lein et al., 2005). Neural stem or progenitor cells, which generate the main cells of the central nervous system (neurons, astrocytes, and oligodendrocytes) are an emerging model for

[☆] Contribution of the U.S. Department of Commerce; not subject to copyright in the U.S.

^{*} Corresponding author. Tel.: +1 303 497 4968; fax: +1 303 497 5030.
E-mail address: jeerage@boulder.nist.gov (K.M. Jeerage).

toxicology (Breier et al., 2010), with many promising results. Rat progenitor cells were more sensitive to methylmercury-induced cytotoxicity than differentiated neural or glial cells (Tamm et al., 2006). Furthermore, cells derived from multiple brain regions responded differently to lead exposure (Huang and Schneider, 2004). Novel human cell models include immortalized progenitor cells (Breier et al., 2008), stem cells derived from umbilical cord blood (Buzanska et al., 2009), and commercially available neurospheres (Fritsche et al., 2005; Moors et al., 2009). Cord blood is a non-controversial source of human stem cells; this model could potentially address the genetic diversity of individuals. Neurospheres resemble the three-dimensional organization of the developing brain, with a proliferative zone of progenitor cells and a zone of maturing neural and glial cells. Altogether, neural progenitor cells are promising models, however investigations to date have focused on proliferation, migration, and differentiation measurements.

Axonal and dendritic outgrowth, or neurite outgrowth, is a defining feature of neural morphology and is critically linked to neural connectivity (Radio and Mundy, 2008). It was recently demonstrated that a chemical which affects neurite outgrowth also affects network function assessed by microelectrode arrays (Robinette et al., 2011). A variety of chemical neurotoxins as well as chemicals regarded as safe (*i.e.*, drugs permitted during pregnancy) have been investigated by high-throughput neurite outgrowth measurements. These experiments employed a variety of cells, including the rat pheochromocytoma (PC-12) cell line (Radio et al., 2008), primary rat cerebellar granule cells (Radio et al., 2010), human embryonic stem-cell-derived neurons (Harrill et al., 2010), and primary rat cortical neurons (Harrill et al., 2011). Other recent developments include substrates for assessing network formation by the human neuroblastoma (SH-SY5Y) cell line (Frimat et al., 2010) and quantitation based on live cell staining (Stiegler et al., 2011).

Neurite outgrowth can be evaluated with cell lines, however the resulting neurites cannot be identified as axons or dendrites and they do not form synapses. Purified cultures of primary neuronal cells also may not adequately represent the *in vivo* environment. In studies of acute cytotoxicity, neuron/astrocyte co-cultures were more resilient than neuronal monocultures (Giordano et al., 2009; Morken et al., 2005; Woehrling et al., 2007, 2010), though astrocytes also metabolize chemicals to their toxic form (Ransom et al., 1987). Astrocytes can inhibit (McKeon et al., 1991) or promote (Oh et al., 2009) neurite outgrowth through the secretion of soluble factors, suggesting that their presence may impact neurite outgrowth assays.

We hypothesize that quantifying neurite outgrowth and differentiation in the same culture may prove valuable for developmental neurotoxicity screening. Lithium was chosen for initial studies. Lithium is widely utilized in the treatment of bipolar disorder, though questions remain about its mode of action (Jope, 1999). *In vitro* studies with neuronal monocultures have shown that lithium interferes with neurite initiation and with neuronal cytoskeletal proteins in chick dorsal root ganglia (Hollander and Bennett, 1991) and rat hippocampal neurons (Takahashi et al., 1999), consistent with recent studies (Harrill et al., 2011). However, studies with neural progenitor cells derived from the rat hippocampus (Kim et al., 2004) or dentate gyrus (Boku et al., 2011) suggest that lithium promotes neurogenesis and suppresses astrogliogenesis. In this work, we examined neurite outgrowth measurements with a commercial rat cortex progenitor cell model in which cells can be exposed to lithium during a period of differentiation. We first examined the influence of seeding density and evaluation timepoint on the expression of neural and glial markers as well as neurite outgrowth. We then evaluated their response to different concentrations of lithium chloride by

quantifying adenosine triphosphate content, neurite outgrowth, and differentiation. Our results support further development of this cell model.

2. Methods¹

2.1. Materials

Rat cortex neural stem/progenitor cells were obtained from Stem Cell Technologies (Vancouver, BC). Cells were isolated from Sprague–Dawley or Fischer 344 rats at E18, where E0 is the day a gestational plug forms. Single cell suspensions were derived from both hemispheres of the cortex, while avoiding the striata and hippocampus. Whole neurospheres were cryopreserved during their first passage after four days of proliferation and supplied in this form. According to the manufacturer, the fraction of cells that differentiate into neurons is strongly influenced by how long the cells have been propagated in neurosphere culture, with early passages having a greater fraction of neurons than later passages. For this reason, our experiments utilized cells passaged exactly twice after isolation and prior to seeding.

The following culture media and growth factors were obtained from Stem Cell Technologies: NeuroCult NS-A proliferation medium, NeuroCult NS-A differentiation medium, recombinant human epidermal growth factor (rhEGF), recombinant human fibroblast growth factor (rhFGF), and heparin. Growth factors were reconstituted according to the manufacturer's protocol with sterile water or phosphate-buffered saline, acetic acid, and bovine-serum albumin. Differentiation medium contained 50 units/mL penicillin and 50 μ g/mL streptomycin (Invitrogen). Cell suspensions were diluted 1:10 to determine cell counts by trypan blue exclusion. All washes and chemical dilutions not otherwise specified were done with Dulbecco's phosphate buffered saline (DPBS).

2.2. Cell culture

Cryopreserved cells were rapidly thawed at 37 °C, then neurospheres were resuspended in proliferation medium containing 20 ng/mL rhEGF, 10 ng/mL rhFGF, and 2 μ g/mL heparin and cultured overnight. After 24 h, the neurospheres were pelleted at 150 \times g, triturated into a single cell suspension, and cultured in proliferation medium with added growth factors. After 48 h, a partial medium change was performed. After an additional 48 h, the neurospheres were pelleted at 150 \times g, resuspended in differentiation medium, triturated into a single cell suspension, counted, and seeded onto 8-well chamber slides (0.8 cm², Lab-Tek) or opaque white 96-well assay plates (0.32 cm², Corning). Cultures surfaces had been previously treated by adding 300 μ L (chamber slide) or 100 μ L (assay plate) of 15 μ g/mL poly-L-ornithine (Sigma–Aldrich) to each chamber and incubating overnight (18 h minimum) to promote cell attachment and differentiation. Wells were triple washed prior to seeding. Cells were initially seeded at 1500 cells/mm², 1250 cells/mm², 1000 cells/mm², 750 cells/mm², 500 cells/mm², and 125 cells/mm² to optimize seeding density for neurite outgrowth evaluation. If the culture period extended to ten days, the medium was partially changed at seven days.

2.3. Chemical exposure

Cells were seeded onto poly-L-ornithine coated surfaces at 1250 cells/mm² (1×10^5 cells/well for chamber slides and

¹ Certain commercial equipment, instruments, or materials are identified in this document. Such identification does not imply recommendation or endorsement by the National Institute of Standards and Technology, nor does it imply that the products identified are necessarily the best available for the purpose.

4×10^4 cells/well for assay plates) and allowed to attach for 4 h prior to chemical exposure. Lithium chloride (Sigma–Aldrich) was diluted in differentiation medium and sterile filtered (0.22 μm polyethersulfone membrane, Corning). A 300 mmol/L stock solution was used to prepare additional stock solutions (100 mmol/L, 30 mmol/L, 10 mmol/L, and 3 mmol/L) by serial dilution. For cells cultured in chamber slides, 50 μL of each stock solution was added to wells containing 450 μL of differentiation medium to give final exposure concentrations of 30 mmol/L, 10 mmol/L, 3 mmol/L, 1 mmol/L, and 0.3 mmol/L. For cells cultured in assay plates, 10 μL of each stock solution was added to wells containing 90 μL of differentiation medium to give the same final exposure concentrations.

2.4. Adenosine triphosphate (ATP) evaluation

ATP levels were evaluated with the CellTiter-Glo Luminescent Cell Viability Assay (Promega). ATP produced by metabolically active cells is detected *via* conversion of luciferin to oxyluciferin in the presence of luciferase enzyme. Individual assay plates were equilibrated at room temperature for 30 min prior to adding the reagent (100 μL /well), which was reconstituted according to the manufacturer's protocol. Plates were mixed at 100 rpm for 2 min on an orbital shaker and then incubated, protected from light, for 10 min at room temperature prior to the reading. Luminescence intensity was measured with a Synergy HT Multimode Plate Reader (Biotek) and corrected for background due to media. We verified that the background-corrected luminescence intensity is linearly proportional ($R^2 = 0.997$) to the number of living cells by measuring wells containing 1×10^3 cells/well, 5×10^3 cells/well, 1×10^4 cells/well, 2×10^4 cells/well, 4×10^4 cells/well, and 6×10^4 cells/well.

2.5. Immunocytochemistry and image acquisition

Cells in chamber slides were fixed by incubation with 4% paraformaldehyde for 30 min at room temperature. Cells were triple-washed, incubated with 0.3% Triton-X 100 for 30 min at room temperature to permeabilize the membrane, then triple-washed again. Fixed cells were incubated with primary antibodies for β -III-tubulin (1:1000) and GFAP (1:500) or nestin (2 $\mu\text{g}/\text{mL}$) for 2 h (37 $^\circ\text{C}$) and with secondary antibodies (1:100–1:150) for 30 min (37 $^\circ\text{C}$), protected from light, with triple-washes after each incubation stage. Cells were then incubated for ~ 90 s with Hoechst 33342 (5 $\mu\text{g}/\text{mL}$) to stain nuclei. Mouse monoclonal antibody for β -III-tubulin (Clone TuJ-1, FitzGerald), rabbit monoclonal antibody for GFAP (Clone EP672Y, Abcam), or mouse monoclonal antibody for nestin (Rat-401 developed by S. Hockfield, Developmental Studies Hybridoma Bank at the University of Iowa) were diluted in DPBS containing 10% normal goat serum. Goat-anti-mouse Alexa Fluor 488 IgG (Invitrogen) and goat-anti-rabbit Alexa Fluor 594 IgG (Invitrogen) were diluted in DPBS containing 2% normal goat serum.

Immunostained cells were imaged with a 20 \times objective on a Nikon TE-2000S inverted microscope equipped with an EXFO X-cite 120 metal-halide arc lamp for epifluorescence illumination. Excitation and emission filters (Omega Optical) were 360/40 nm excitation and 460/50 nm emission for Hoechst 33342, 480/30 nm excitation and 535/40 emission for AlexaFluor 488, and 560/55 nm excitation and 645/75 nm emission for AlexaFluor 594. All images were captured by a 12-bit monochrome camera (Photometrics ES2) with Metamorph Software (Molecular Devices). Integration periods were fixed for each series of wells and were determined by sampling control wells from multiple slides. Images shown in figures have consistent acquisition conditions and intensity scales.

2.6. Neurite outgrowth evaluation

Neurons were identified by β -III-tubulin positive neurites extending from a cell body (Hoechst 33342 positive) that was bounded by β -III-tubulin. Neurites were traced on a cell-by-cell basis with the NeuronJ plugin for ImageJ (Meijering et al., 2004) or on an image-average basis with NeuroLucida (MBF Biosciences). Example traces illustrate the main differences between these two tracing methods (Fig. 1). When traced on a cell-by-cell basis, neurites were traced from each cell body. Neurons with off-image neurites were excluded, as were neurites whose cell body could not be identified. Ambiguities due to crossing neurites were resolved by the observer, when judged possible, otherwise the entire cluster of neurons was excluded. When traced on an image-average basis, neurites were traced through the cell body because automatic detection of cell bodies was inconsistent, depending on

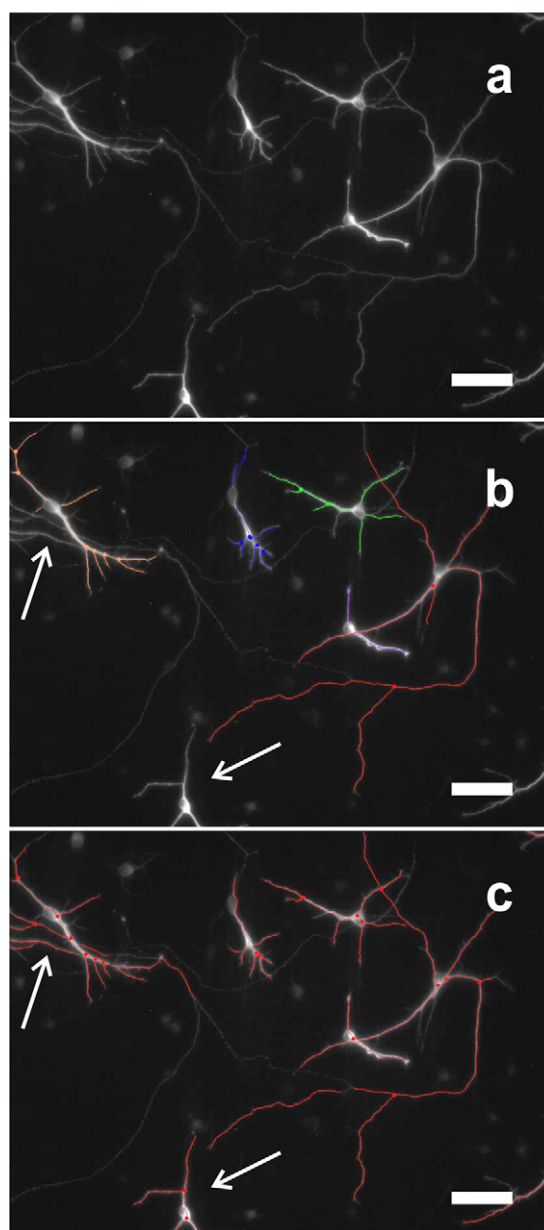


Fig. 1. β -III-tubulin image scaled for contrast (a) with semi-automated neurite tracing on a cell-by-cell basis (b) or fully automated neurite tracing on an image-average basis (c). Scale bars are 50 μm . Arrows indicate neurites or neurons which were excluded in (b) because their cell body or neurites were off image.

the extent of staining. All neurites were traced and there was no need to resolve ambiguities.

In NeuronJ, each series of 12-bit β -III-tubulin images was scaled to increase contrast, then converted to 8-bit images, which is the required format. Multiple images were examined to choose an intensity scale that was applied to all images. Only processes greater than 10 μm in length were identified as neurites and included in neurite counts or length measurements. Three measurements were made: neurites per cell, longest neurite per cell, which does not include secondary or tertiary branches, and neurite outgrowth per cell, which includes all branches. These cell-level measurements were averaged to determine the value for each well.

In NeuroLucida, each series of 12-bit β -III-tubulin images was again consistently scaled. When images were scaled to provide better contrast with no loss of information, the traced lengths were greater than for unscaled images. This is because, for our acquisition conditions, even the brightest neurons only required about half the intensity range. Fully automated tracing employed consistent settings for seed placement and gap tolerance. For each image traced, neurons were identified by observation as previously described. Neurite outgrowth was summed for all images and divided by the total number of identified neurons to determine the value for each well.

2.7. Statistical analysis

All statistical analysis was performed with InStat (GraphPad Software). Each well was considered an individual sample and mean values are reported plus or minus standard error of the mean. To determine the fractions of immunopositive progenitors, neurons, or astrocytes, at least 500 cells were scored per well. When individual neurites were traced (Neuron J), 4–10 images were analyzed per well. Typically 25–35 neurons were evaluated, however, at the low densities (125–500 cells/ mm^2) studied in Fig. 3, two wells per timepoint had fewer than 25 neurons after all images were analyzed. When neurites were traced on an average basis (NeuroLucida), 9 or 10 images were analyzed per well, with an average of 80 neurons (minimum of 50 neurons) identified per well. Results from individual cultures were normalized by controls from that culture and then combined with normalized values from other cultures. Student's *t*-test was employed for comparisons between two groups. For three or more groups, means were compared by one-way analysis of variance (ANOVA) with $p < 0.05$ considered significant. Each pair of means was then evaluated by the Student–Newman–Keuls post-test to determine if cultures were significantly different from controls or from each other.

3. Results and discussion

3.1. Neuronal differentiation and outgrowth

Immediately after seeding the cells appeared spherical, but they rapidly attached to poly-L-ornithine coated surfaces. Four hours after seeding, short extensions were visible in some cells. After three days in culture, thin processes extended from a large fraction of cells. There were also clusters of apparently dead cells. From this point, the cultures did not change dramatically in appearance. However, they did become challenging to examine with phase contrast optics, because processes extending from the cells began to overlap with those from other cells. After ten days in culture, there appeared to be a larger fraction of dead cells, though we did not quantify this with viability assays.

Neural differentiation and outgrowth were examined five days (d5), seven days (d7), and ten days (d10) after seeding by immunocytochemical staining for β -III-tubulin, a microtubule

protein that is present in axons, dendrites, and in the cell body (Fig. 2). Based on the original seeding densities, the average number of cells in a single ($20\times$) image is 200 cells/image (1250 cells/ mm^2), 100 cells/image (750 cells/ mm^2), or 20 cells/image (125 cells/ mm^2). Only a portion of each image is shown in Fig. 2, but the increase in cell–cell spacing from 1250 cells/ mm^2 to 125 cells/ mm^2 is clear in the nuclear images.

β -III-tubulin positive cells were observed on d5 for all seeding densities. Neurites appeared to increase in length and branching from d5 to d7 and from d7 to d10. Cells cultured for fourteen days or longer had long, branching neurites that could not be analyzed on a cell-by-cell basis due to numerous ambiguities as neurites cross. Higher seeding densities appeared to promote greater outgrowth, which was quantified by two parameters: number of neurites per cell and longest neurite per cell (Fig. 3). The majority of cells in these cultures were not neurons. Cell bodies that were faintly outlined with β -III-tubulin, but did not possess a process longer than 10 μm in length, were not identified as neurons. Therefore all neurons had at least one neurite. Seeding density did not impact the number of neurites per cell at any timepoint (Fig. 3a). Two to four neurites were typically identified per neuron and though this measure does increase significantly with time, the increase is only by one-third.

Longest neurite per cell was influenced by seeding density and timepoint (Fig. 3b). For cells seeded at high densities (1250–1500 cells/ mm^2), neurite length increased significantly from d5 to d7 and from d7 to d10, approximately doubling overall. Cells seeded at intermediate (750–1000 cells/ mm^2) or low densities (125–500 cells/ mm^2) also had significant increases in neurite length with time, however neurites were significantly shorter on d10 compared to high density cultures. Altogether, our results indicate that longest neurite per cell is more sensitive to culture parameters than neurites per cell. We chose 1250 cells/ mm^2 as the seeding density for all further studies to ensure consistent neurite outgrowth with time, maximize neurite length, and minimize the possibility that local variation in cell–cell spacing could cause changes in neurite outgrowth.

3.2. Development of the progenitor cell culture

We examined the expression of glial fibrillary acidic protein, an intermediate filament protein that indicates astrocytes, but is also expressed by other cells of the central nervous system. In preliminary studies, we observed very few astrocytes in cultures seeded at low densities, even on d10, whereas cultures seeded at high densities had abundant expression (data not shown). For cultures seeded at 1250 cells/ mm^2 , the seeding density employed for all further studies described here, immunocytochemical staining suggests that expression of this protein increases dramatically between d7 and d10 (Fig. 4). Examining the d10 image also shows that cells in this culture either express a neuronal or an astrocytic phenotype, as opposed to an intermediate phenotype.

In rat cortex tissue, the ratio of astrocytes to neurons is 1–3 (Nedergaard et al., 2003). Unlike studies in which purified populations of neurons and astrocytes are combined to yield neural/glial cultures with defined cellular ratios (Woehrling et al., 2010), the cellular ratios in this study were dictated solely by differentiation of the progenitor cell culture. Cultures evaluated at multiple timepoints show that both the fraction of neurons and the fraction of astrocytes increased significantly from d3 to d10 (Fig. 5a). While the fraction of neurons doubled, the fraction of astrocytes increased by a factor of more than twenty, with about 75% of the increase occurring between d7 and d10. As a result, the ratio of astrocytes to neurons also increased significantly with time (Table 1). Other researchers have demonstrated that seeding

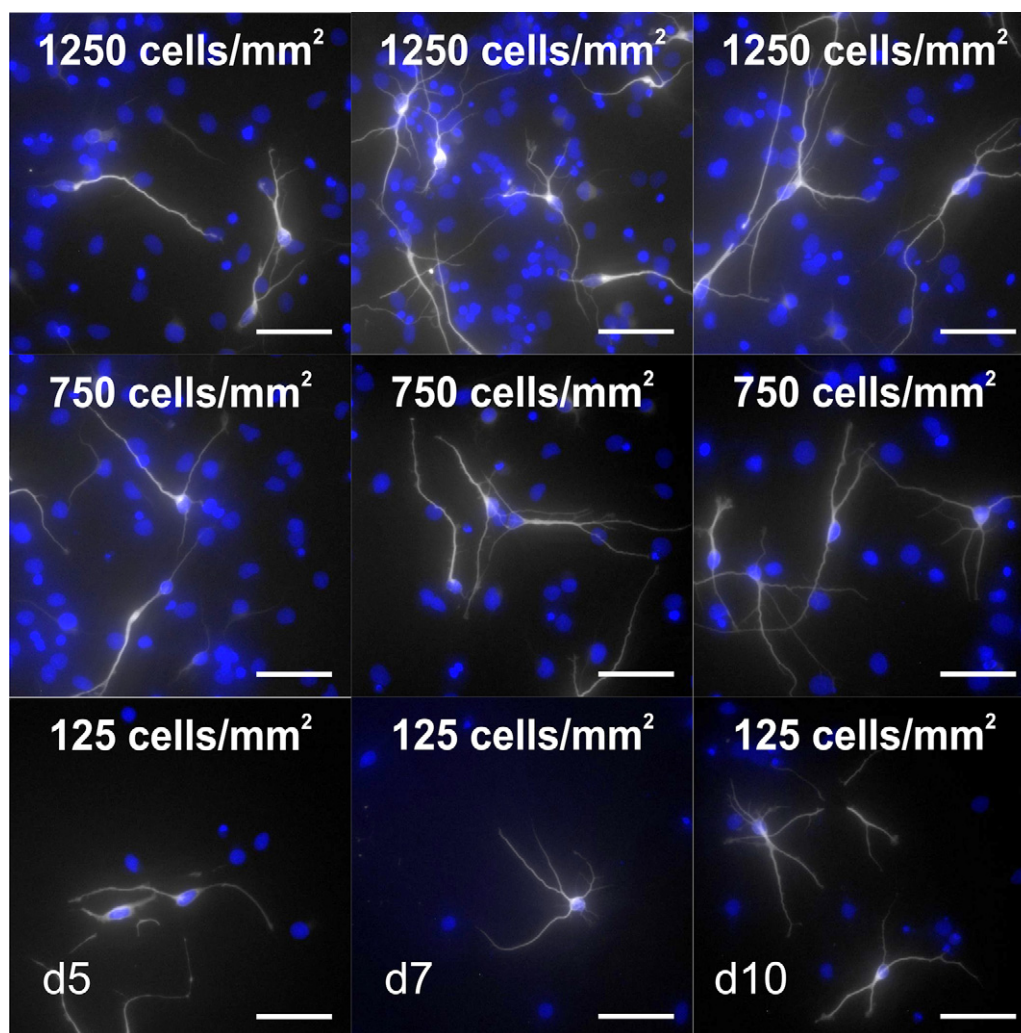


Fig. 2. Images of neurons (β -III-tubulin, white) as a function of seeding density and evaluation timepoint. Hoechst-stained nuclei are blue and scale bars are 50 μ m. (For interpretation of the references to color in this figure caption, the reader is referred to the web version of the article.)

neural stem or progenitor cells onto stiff substrates promotes astrocyte differentiation over neural differentiation (Lampe et al., 2010; Saha et al., 2008), so the high ratio of astrocytes to neurons may be a consequence of the polystyrene culture surface.

Nestin is an intermediate filament protein expressed during the early stages of development and is a marker of progenitor cells. Cultures evaluated at multiple timepoints show that the fraction of progenitor cells decreased significantly from d3 to d10 (Fig. 5b). The cell fractions in Fig. 5a and b, sum to within 8% of 100% on d3, d5, and d7. On d10, the sum is 110%, so it is likely that many cells scored as astrocytes still expressed nestin. Altogether, these results indicate that the cultures are developing from a predominantly progenitor cell population on d3, to a population with a significant fraction of neurons and astrocytes on d10.

3.3. ATP content of cultures exposed to LiCl

Adenosine triphosphate (ATP) content in neural progenitor cell cultures had a concentration-dependent response to LiCl exposure (Fig. 6). 30 mmol/L LiCl reduced ATP content by more than 90% on d3 and d5 whereas 10 mmol/L LiCl reduced ATP content by 35% on d3 and 70% on d5. Additional timepoints on d7 and d10 were similar to d5 (averages from six wells, data not shown). Specifically, cultures exposed to 10 mmol/L LiCl still had non-zero ATP content. Cultures with lower LiCl exposures (3–0.3 mmol/L)

were not significantly different from control cultures at any timepoint, including d7 and d10. Our results for 30 mmol/L and 10 mmol/L LiCl exposures are consistent with Harrill et al. (2010) who also reported decreases in ATP content at these concentrations with human embryonic stem-cell-derived neurons. However, we observed greater differences from control at either concentration, likely reflecting the longer exposure period (3–10 days vs. 24 h) or greater sensitivity of the progenitor cell population. Mature neural/glial cultures exposed for three days had a half-maximal inhibitory concentration greater than 32 mmol/L LiCl (Woehrling et al., 2010), so again the rat cortex progenitor cell population appears quite sensitive.

Normal functioning of the central nervous system requires significant energy resources and neurotoxins often impact mitochondrial function (Massicotte et al., 2005). The dramatic decreases in ATP content observed on d3, d5, d7, and d10 suggest that cultures exposed to 30 mmol/L or 10 mmol/L LiCl may contain few viable cells on d10. To examine this, we employed Live/Dead staining with calcein acetoxymethyl ester (indicates intact cells with esterase activity) and ethidium homodimer-1 (indicates dead cells with compromised membranes). Cultures exposed to 30 mmol/L LiCl were sparsely populated, apparently most cells detached from the surface. Of the remaining cells, some live cells were observed, but they were rounded. Cultures exposed to 10 mmol/L LiCl had clusters of live cells interspersed with dead

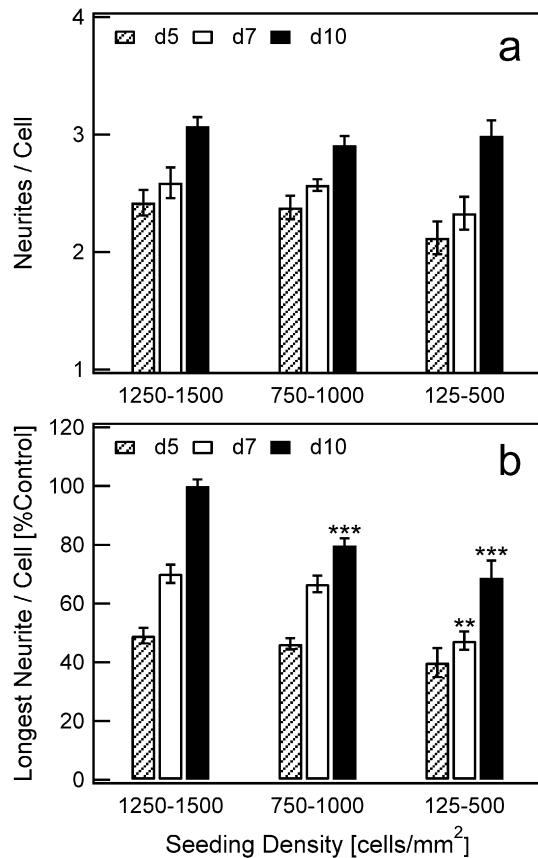


Fig. 3. Neurites per cell (a) and longest neurite per cell (b) as a function of seeding density and evaluation timepoint. To normalize longest neurite per cell, d10 measurements at high densities (1250–1500 cells/mm²) were treated as controls. Reported values are based on 8 wells from two independent cultures and error bars indicate standard error of the mean. ANOVA indicates that both measurements increase significantly with time for all seeding densities ($p < 0.005$). In (a), the number of neurites per cell is not significantly affected by seeding density. In (b), the longest neurite per cell is significantly affected by seeding density on d7 ($p < 0.002$) and d10 ($p < 0.0001$). Stars indicate significant differences from high densities (1250–1500 cells/mm²) in post-test comparisons (** $p < 0.01$ and *** $p < 0.001$).

cells and large regions containing primarily dead cells. Cultures with lower LiCl exposures (3–0.3 mmol/L) contained dense populations of live cells interspersed with dead cells. These cultures could not be distinguished from control cultures by observation.

Culture-level measurements such as ATP content are dominated by progenitor cells throughout this study, since our cultures still consist primarily of progenitor cells on d10 (Fig. 5b). As such, it cannot be determined whether LiCl exposure preferentially kills neurons or astrocytes through ATP content measurements. In order to more effectively track the viability of these minority cell types, cultures exposed to 3 mmol/L LiCl were scored for neuronal and astrocytic differentiation on d10 and compared to control cultures (Table 2). Based on the observed cell fractions, we conclude that 3 mmol/L LiCl exposure does not specifically reduce neuron or astrocyte viability.

3.4. Neurite outgrowth in cultures exposed to LiCl

Following immunocytochemical staining on d10, cultures exposed to 30 mmol/L or 10 mmol/L LiCl had very few nuclei of normal size and distribution. Instead, clusters of small bright nuclei, corresponding to dead cells, were observed. No β -III-tubulin positive neurons were observed under either exposure

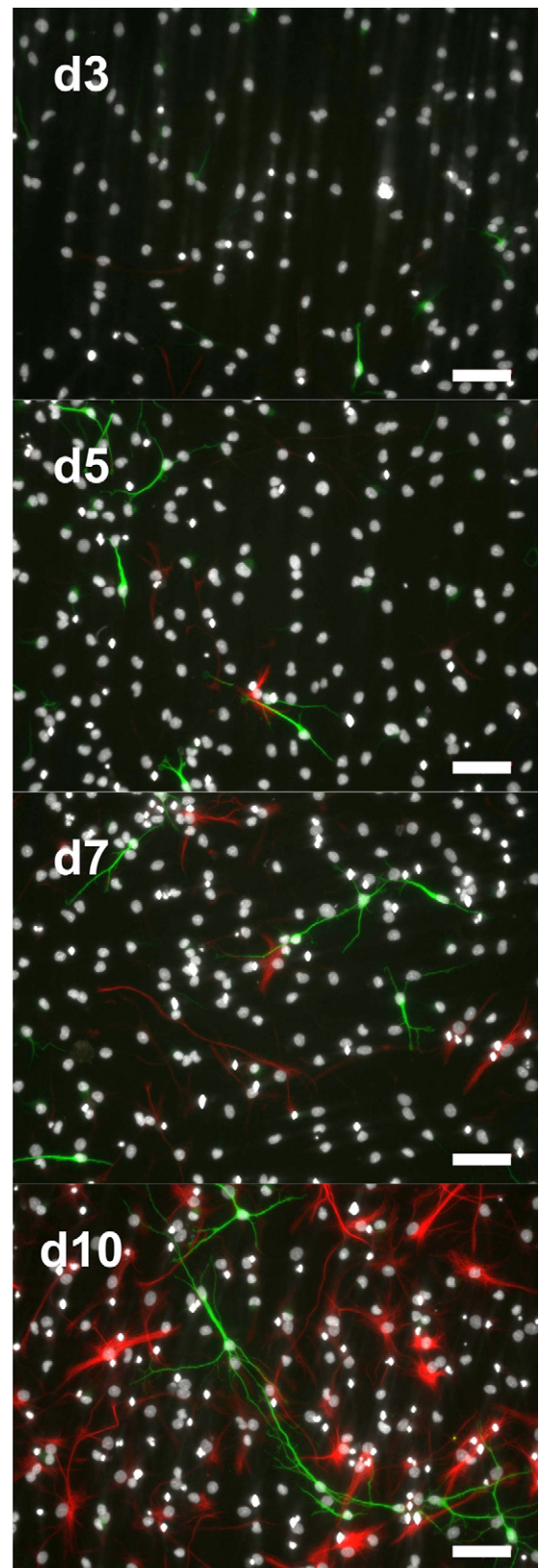


Fig. 4. Images of neurons (β -III-tubulin, green) and astrocytes (glial fibrillary acidic protein, red) as a function of evaluation timepoint. Hoechst-stained nuclei are white and scale bars are 50 μ m. (For interpretation of the references to color in this figure caption, the reader is referred to the web version of the article.)

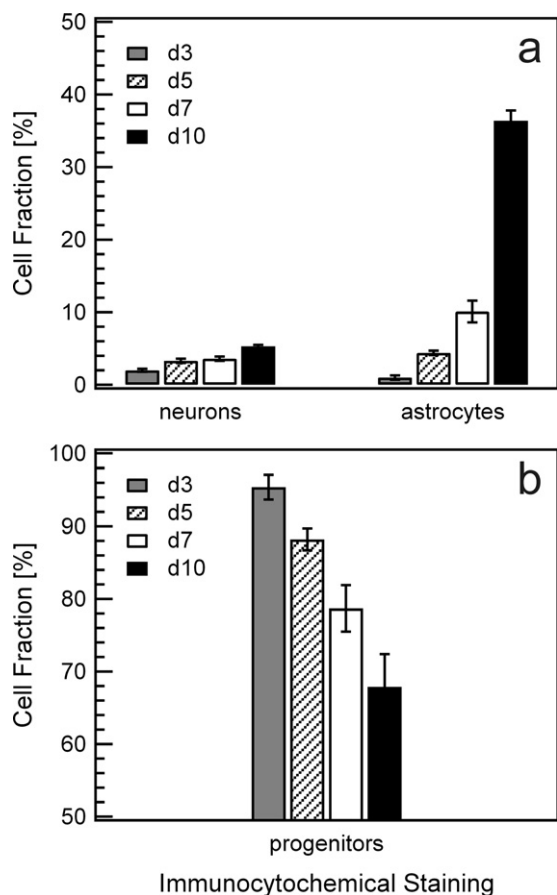


Fig. 5. Neuron and astrocyte fractions (a) and progenitor cell fractions (b) as a function of evaluation timepoint. Reported values are based on 10 wells from two independent cultures, with the exception of neuron and astrocyte fractions on d10, which are based on 26 wells from five independent cultures. Error bars indicate standard error of the mean. Separate wells were utilized for quantifying progenitor cells vs. neurons and astrocytes. ANOVA indicates that the fractions of neurons and astrocytes increase with time ($p < 0.0001$ for both) whereas the fraction of progenitor cells decreases with time ($p < 0.0001$).

condition and these cultures could not be evaluated further. In contrast, cultures exposed to 3 mmol/L, 1 mmol/L, and 0.3 mmol/L LiCl appeared similar to control cultures, with comparable numbers of β -III-tubulin positive neurons observed in each image. Neurite outgrowth for these LiCl concentrations was first evaluated on a cell-by-cell basis (Neuron), Fig. 7a and b) and then on an image-average basis (NeuroLucida, Fig. 7c).

Fig. 7a and b allows us to compare measurements of longest neurite per cell with neurite outgrowth per cell. We found that normalized values were not significantly different from each other for any LiCl exposure. However, tracing neurites on a cell-by-cell basis requires fairly isolated cells and is only possible in this culture because the fraction of neurons is low. Because some

Table 1

Astrocyte to neuron ratio at multiple timepoints. Reported values (and standard error of the mean) are based on 10 wells from two independent cultures for d3, d5, and d7 and 26 wells from five independent cultures for d10.

Timepoint	Astrocyte:neuron
d3	0.8 ± 0.1
d5	1.5 ± 0.2
d7	3.3 ± 0.7
d10	7.5 ± 0.6

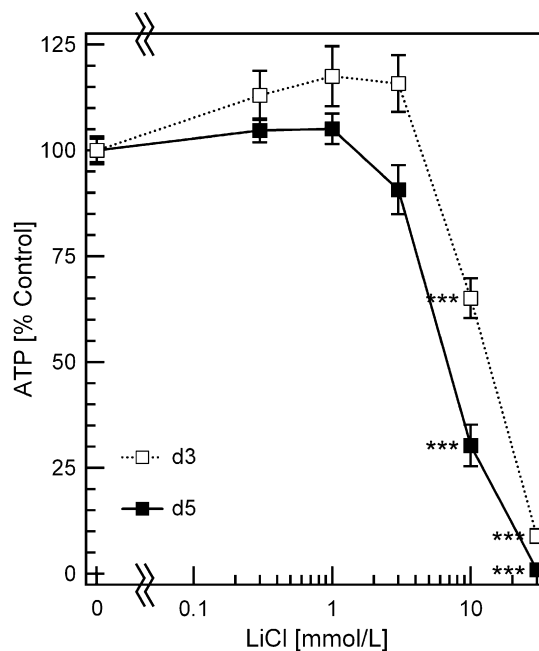


Fig. 6. Adenosine triphosphate content of cultures exposed to LiCl until evaluation on d3 or d5. Reported values are based on 12 wells from two independent cultures and error bars indicate standard error of the mean. Stars indicate significant differences from controls in post-test comparisons ($***p < 0.001$).

ambiguities were resolved by observation and cell clusters were excluded from analysis, it also has the potential to be biased. By contrast, fully automated tracing on an image-average basis includes all neurites in an image and is rapid, allowing more wells to be evaluated. Prior to evaluating the effects of LiCl exposure, we verified that neurite outgrowth per cell, determined on an image-average basis, increased from d5 to d7 and d7 to d10 by evaluating the images used to generate Fig. 5a (data not shown). These results matched the results already described in Fig. 3b and provide confidence in this methodology. Similar to the preliminary measurements in Fig. 7a and b, measurements of neurite outgrowth per cell in Fig. 7c indicate a concentration-dependent decrease in neurite outgrowth in response to LiCl exposure, with sensitivity to 0.3 mmol/L LiCl. Interestingly, this is lower than the approximate therapeutic concentration (1 mmol/L Li^+) (Jope, 1999).

Neurons in rat cortex progenitor cell cultures appear sensitive to lower LiCl concentrations than other cultures which have been studied. Harrill et al. observed decreases in neurite outgrowth in human embryonic stem-cell-derived neurons and primary rat cortical neurons at 10 mmol/L. These studies are comparable because the same parameter, neurite outgrowth per cell, was evaluated. However, the exposure period studied here was much longer, resulting in about 300 μm of outgrowth per neuron in d10 control cultures. Other studies with various approaches to neurite outgrowth evaluation (e.g., neurite bed density, axon length) reported inhibition at concentrations as low as 2 mmol/L.

Table 2

Neuron and astrocyte fractions on d10 as a function of LiCl exposure. Reported values (and standard error of the mean) are based on 26 wells from five independent cultures.

Differentiation	LiCl (mmol/L)	Cell fraction (%)	Student's <i>t</i> -test
Neurons	0	5.3 ± 0.2	$p < 0.02$
	3	6.3 ± 0.3	
Astrocytes	0	36.4 ± 1.4	$p < 0.01$
	3	31.3 ± 1.1	

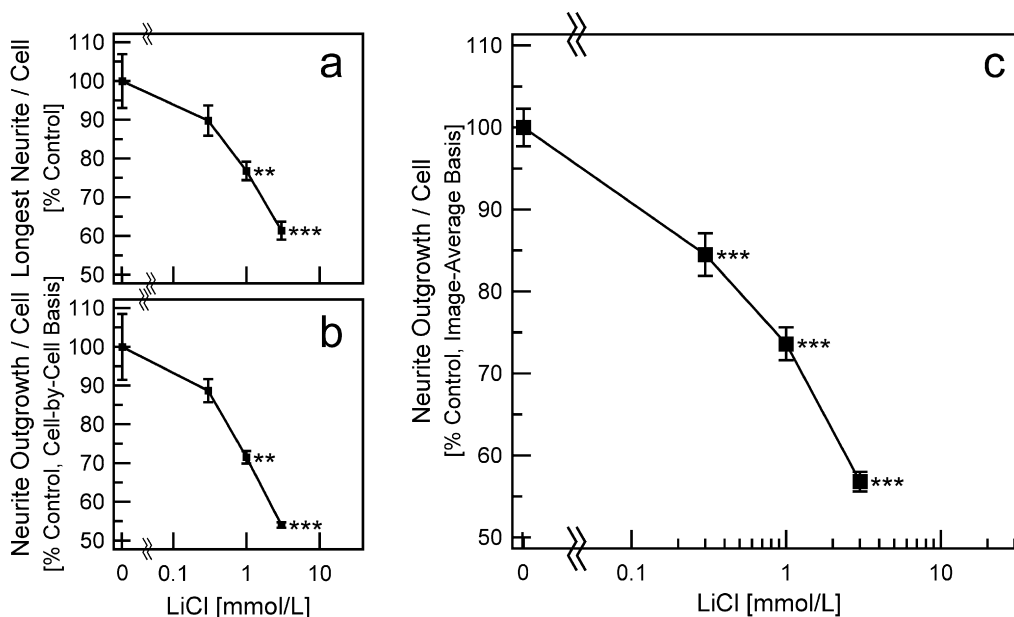


Fig. 7. Longest neurite per cell (a), neurite outgrowth per cell determined on a cell-by-cell basis (b), and neurite outgrowth per cell determined on an image-average basis (c) in cultures exposed to LiCl until evaluation on d10. Reported values are based on 4 wells from one culture in (a) and (b) and 16 wells from three additional, independent cultures in (c). Error bars indicate standard error of the mean and stars indicate significant differences from controls in post-test comparisons (** $p < 0.01$ and **** $p < 0.001$).

Interestingly, Harrill et al. reported that for human embryonic stem-cell-derived neurons, there were no LiCl concentrations that decreased neurite outgrowth without simultaneous indications of cytotoxicity (Harrill et al., 2010). For primary rat cortical neurons, 10 mmol/L LiCl decreased neurite outgrowth without cytotoxicity (Harrill et al., 2011). Our results are consistent with this finding.

In a separate experiment, we examined neurite outgrowth per cell as a function of timepoint and chemical exposure (Fig. 8), choosing 3 mmol/L LiCl exposure, which had the greatest effect on neurite outgrowth, without affecting overall viability. Interestingly, cultures evaluated after five days of exposure to 3 mmol/L LiCl had the same neurite outgrowth as control cultures. Furthermore, cultures exposed to 3 mmol/L LiCl showed an increase in neurite outgrowth from d5 to d10, as did control cultures. However, the magnitude of the increase was quite different. Control cultures more than doubled their neurite outgrowth from d5 to d10,

whereas cultures exposed to 3 mmol/L LiCl increased their neurite outgrowth by about one-third. As a result, cultures evaluated after ten days of exposure to 3 mmol/L LiCl had significantly less neurite outgrowth than control cultures.

Studies with neural progenitor cells derived from the rat hippocampus (Kim et al., 2004) found that LiCl promotes neurogenesis and reduces astroglialgenesis, whereas progenitors derived from the rat dentate gyrus required retinoic acid and LiCl to achieve the same effect (Boku et al., 2011). This literature suggests the possibility that the effects of LiCl exposure reported here derive from an increase in the number of immature neurons rather than inhibition of neurite outgrowth. We examined this possibility by quantifying the fraction of differentiated neurons and astrocytes in cultures exposed to 3 mmol/L LiCl (Table 2). Our data provides evidence for neurogenesis (20% increase) and suppression of astroglialgenesis (13% decrease). However, results for individual cultures were variable. Individual cultures exhibited non-significant increases in neuron fractions (coefficient of variance of 7.3% between biological replicates). Two cultures exhibited significant decreases in astrocyte fractions, the other three cultures did not (coefficient of variance of 16.4% between biological replicates). In contrast, decreases in neurite outgrowth (from Figs. 7 and 8) were consistent and statistically significant for each individual culture. For developmental neurotoxicity screening, alterations in either differentiation or neurite outgrowth could prioritize a chemical for additional studies. Our results suggest that measurement of neurite outgrowth is more robust.

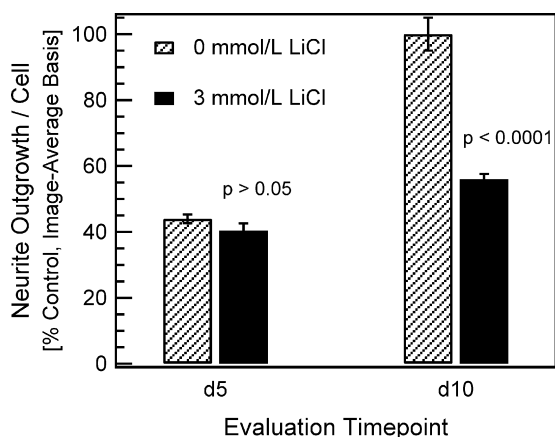


Fig. 8. Neurite outgrowth per cell determined on an image-average basis in cultures exposed to LiCl until evaluation on d5 or d10. Reported values (normalized to control cultures on d10) are based on 10 wells from two independent cultures and error bars indicate standard error of the mean. Student's *t*-test indicates that 3 mmol/L LiCl does not significantly impact neurite outgrowth on d5, but differences are significant on d10 (p values reported in figure).

3.5. Culture to culture variability

A significant concern for toxicity screening is the potential for culture-to-culture variability. While the focus of this work was to investigate neurite outgrowth and differentiation with a commercially available rat cortex progenitor cell model, our results provide preliminary evidence that this cell model behaves in a reproducible manner. Nine independent cultures were used in these studies. Since any individual culture provides a limited quantity of cells, every endpoint could not be evaluated at each timepoint. Longest neurite per cell was measured in Figs. 3b and 7a, and raw values for

the d10 control cultures ($113 \pm 9 \mu\text{m}$ per cell and $115 \pm 8 \mu\text{m}$ per cell, respectively) were quite similar. Despite the different tracing methodologies employed, raw values of neurite outgrowth per cell for the control cultures in Figs. 7b, c and 8 were also quite similar ($291 \pm 25 \mu\text{m}$ per cell, $308 \pm 15 \mu\text{m}$ per cell, and $296 \pm 15 \mu\text{m}$ per cell, respectively). Exposure to 3 mmol/L LiCl, in particular, led to very consistent decreases in neurite outgrowth per cell in six independent cultures, with a coefficient of variance of 6.1% between biological replicates. Altogether, these studies indicate that rat cortex progenitor cells are a promising candidate for future studies aimed at developing reproducible models for developmental neurotoxicity screening.

4. Conclusions

Rat cortex neural progenitor cells differentiated into a population of about 5% neuronal and 36% astroglial cells after ten days in culture. Culture-level measurements of adenosine triphosphate content indicated that exposure to 10 mmol/L or 30 mmol/L lithium chloride was cytotoxic, whereas lower concentrations were not cytotoxic. Since culture-level measurements were dominated by progenitor cells at all timepoints, this result was supported by quantifying neuronal and astroglial populations. Cultures exposed to 0.3–3 mmol/L lithium chloride exhibited concentration-dependent decreases in neurite outgrowth by multiple tracing methodologies. Decreases in neurite outgrowth were observed after ten days of exposure, whereas five days of exposure were insufficient to produce an effect. This work demonstrates that neurite outgrowth in differentiating progenitor cell cultures can be a sensitive endpoint at non-cytotoxic exposures. Rat cortex progenitor cells are a promising model for future studies of the connection between differentiation and neurite outgrowth endpoints, axonal vs. dendritic outgrowth, and reproducibility for developmental neurotoxicity screening.

Conflict of interest statement

The authors declare that there are no conflicts of interest.

Role of the funding source

This research was supported by internal NIST funding. The manuscript was reviewed and approved by the NIST Editorial Review Board prior to submission.

Acknowledgements

T. Oreskovic is supported by a NIST-ARRA Fellowship and S. Hume is supported by a National Research Council (NRC) Postdoctoral Fellowship. N. Goldstein provided assistance with immunocytochemical staining and image acquisition. The authors would like to thank three anonymous reviewers for their detailed comments, which led to important improvements in the final manuscript.

References

- Bal-Price AK, Hogberg HT, Buzanska L, Coecke S. Relevance of in vitro neurotoxicity testing for regulatory requirements: challenges to be considered. *Neurotoxicol Teratol* 2010;32(1):36–41.
- Barone S, Das KP, Lassiter TL, White LD. Vulnerable processes of nervous system development: a review of markers and methods. *Neurotoxicology* 2000;21(1–2):15–36.
- Berger-Sweeney J, Hohmann CF. Behavioral consequences of abnormal cortical development: insights into developmental disabilities. *Behav Brain Res* 1997;86:121–42.
- Boku S, Nakagawa S, Masuda T, Nishikawa H, Kato A, Toda H, et al. Effects of mood stabilizers on adult dentate gyrus-derived neural precursor cells. *Progr Neuro-Psychopharmacol Biol Psychiatry* 2011;35(1):111–7.
- Breier J, Gassmann K, Kayser R, Stegeman H, De Groot D, Fritsche E, et al. Neural progenitor cells as models for high-throughput screens of developmental neurotoxicity: state of the science. *Neurotoxicol Teratol* 2010;32(1):4–15.
- Breier J, Radio N, Mundy W, Shafer T. Development of a high-throughput screening assay for chemical effects on proliferation and viability of immortalized human neural progenitor cells. *Toxicol Sci* 2008;105(1):119–33.
- Buzanska L, Sypecka J, Nerini-Molteni S, Compagnoni A, Hogberg HT, del Torchio R, et al. A human stem cell-based model for identifying adverse effects of organic and inorganic chemicals on the developing nervous system. *Stem Cells* 2009;27(10):2591–601.
- Crofton KM, Mundy WR, Lein PJ, Bal-Price AK, Coecke S, Seiler AEM, et al. Developmental neurotoxicity testing: recommendations for developing alternative methods for the screening and prioritization of chemicals. *ALTEX* 2011;28:9–15.
- Frimat J-P, Sisnaise J, Subanatarajan S, Menne H, Godoy P, Lampen P, et al. The network formation assay: a spatially standardized neurite outgrowth analytical display for neurotoxicity screening. *Lab Chip* 2010;10(6):701–9.
- Fritsche E, Cline J, Nguyen N, Scanlan T, Abel J. Polychlorinated biphenyls disturb differentiation of normal human neural progenitor cells: clue for involvement of thyroid hormone receptors. *Environ Health Perspect* 2005;113(7):871–6.
- Giordano G, Kavanagh J, Costa LG. Mouse cerebellar astrocytes protect cerebellar granule neurons against toxicity of the polybrominated diphenyl ether (PBDE) mixture DE-71. *Neurotoxicology* 2009;30(2):326–9.
- Goldman LR, Koduru S. Chemicals in the environment and developmental toxicity to children: a public health and policy perspective. *Environ Health Perspect* 2000;108(3):443–8.
- Grandjean P, Landrigan PJ. Developmental neurotoxicity of industrial chemicals. *Lancet* 2006;368(9553):2167–78.
- Harrill J, Freudenrich T, Machacek D, Stice S, Mundy W. Quantitative assessment of neurite outgrowth in human embryonic stem cell-derived hN2 (TM) cells using automated high-content image analysis. *Neurotoxicology* 2010;31(3):277–90.
- Harrill JA, Freudenrich TM, Robinette BL, Mundy WR. Comparative sensitivity of human and rat neural cultures to chemical-induced inhibition of neurite outgrowth. *Toxicol Appl Pharmacol* 2011;256(3):268–80.
- Harry CJ, Billingsley M, Bruinink A, Campbell IL, Classen W, Dorman DC, et al. In vitro techniques for the assessment of neurotoxicity. *Environ Health Perspect* 1998;106:131–58.
- Harry CJ, Tiffany-Castiglioni E. Evaluation of neurotoxic potential by use of in vitro systems. *Expert Opin Drug Metab Toxicol* 2005;1(4):701–13.
- Hollander BA, Bennett GS. Lithium chloride alters cytoskeletal organization in growing, but not mature, cultured chick sensory neurons. *J Neurosci Res* 1991;28(3):332–42.
- Huang F, Schneider J. Effects of lead exposure on proliferation and differentiation of neural stem cells derived from different regions of embryonic rats brain. *Neurotoxicology* 2004;25(6):1001–12.
- Jope RS. Anti-bipolar therapy: mechanism of action of lithium. *Mol Psychiatry* 1999;4(2):117–28.
- Kim JS, Chang MY, Yu IT, Kim JH, Lee SH, Lee YS, et al. Lithium selectively increases neuronal differentiation of hippocampal neural progenitor cells both in vitro and in vivo. *J Neurochem* 2004;89(2):324–36.
- Lampe K, Mooney R, Bjugstad K, Mahoney M. Effect of macromer weight percent on neural cell growth in 2D and 3D nondegradable PEG hydrogel culture. *J Biomed Mater Res Part A* 2010;94A(4):1162–71.
- Lein P, Locke P, Goldberg A. Alternatives for developmental neurotoxicity testing. *Environ Health Perspect* 2007;115(5):764–8.
- Lein P, Silbergeld E, Locke P, Goldberg AM. In vitro and other alternative approaches to developmental neurotoxicity testing (DNT). *Environ Toxicol Pharmacol* 2005;19(3):735–44.
- Massicotte C, Knight K, Van Der Schyf CJ, Jortner BS, Ehrlich M. Effects of organophosphorus compounds on ATP production and mitochondrial integrity in cultured cells. *Neurotox Res* 2005;7(3):203–17.
- McKeon RJ, Schreiber RC, Rudge JS, Silver J. Reduction of neurite outgrowth in a model of glial scarring following CNS injury is correlated with the expression of inhibitory molecules on reactive astrocytes. *J Neurosci* 1991;11(11):3398–411.
- Meijering E, Jacob M, Sarria JCF, Steiner P, Hirling H, Unser M. Design and validation of a tool for neurite tracing and analysis in fluorescence microscopy images. *Cytometry Part A* 2004;58A(2):167–76.
- Moors M, Rockel TD, Abel J, Cline JE, Gassman K, Schreiber T, et al. Human neurospheres as three-dimensional cellular systems for developmental neurotoxicity testing. *Environ Health Perspect* 2009;117(7):1131–8.
- Morken TS, Sonnewald U, Aschner M, Syversen T. Effects of methylmercury on primary brain cells in mono- and co-culture. *Toxicol Sci* 2005;87(1):169–75.
- Nedergaard M, Ransom B, Goldman SA. New roles for astrocytes: redefining the functional architecture of the brain. *Trends Neurosci* 2003;26(10):523–30.
- Oh J, Recknor JB, Recknor JC, Mallapragada SK, Sakaguchi DS. Soluble factors from neocortical astrocytes enhance neuronal differentiation of neural progenitor cells from adult rat hippocampus on micropatterned polymer substrates. *J Biomed Mater Res A* 2009;91(2):575–85.
- Radio N, Breier J, Shafer T, Mundy W. Assessment of chemical effects on neurite outgrowth in PC12 cells using high content screening. *Toxicol Sci* 2008;105(1):106–18.
- Radio N, Freudenrich T, Robinette B, Crofton K, Mundy W. Comparison of PC12 and cerebellar granule cell cultures for evaluating neurite outgrowth using high content analysis. *Neurotoxicol Teratol* 2010;32(1):25–35.
- Radio N, Mundy W. Developmental neurotoxicity testing in vitro: models for assessing chemical effects on neurite outgrowth. *Neurotoxicology* 2008;29(3):361–76.

- Ransom BR, Kunis DM, Irwin I, Langston JW. Astrocytes convert the parkinsonian inducing neurotoxin, MPTP, to its active metabolite, MPP+. *Neurosci Lett* 1987;75(3):323–8.
- Robinette B, Harrill JA, Mundy WR, Shafer TJ. In vitro assessment of developmental neurotoxicity: use of microelectrode arrays to measure functional changes in neuronal network ontogeny. *Front Neuroeng* 2011;4:1–8.
- Rodier PM. Developing brain as a target of toxicity. *Environ Health Perspect* 1995;103:73–6.
- Saha K, Keung AJ, Irwin EF, Li Y, Little L, Schaffer DV, et al. Substrate modulus directs neural stem cell behavior. *Biophys J* 2008;95(9):4426–38.
- Stiegler NV, Krug AK, Matt F, Leist M. Assessment of chemical-induced impairment of human neurite outgrowth by multiparametric live cell imaging in high-density cultures. *Toxicol Sci* 2011;121(1):73–87.
- Takahashi M, Yasutake K, Tomizawa K. Lithium inhibits neurite growth and tau protein kinase I/glycogen synthase kinase-3beta-dependent phosphorylation of juvenile tau in cultured hippocampal neurons. *J Neurochem* 1999;73(5):2073–83.
- Tamm C, Duckworth J, Hermanson O, Ceccatelli S. High susceptibility of neural stem cells to methylmercury toxicity: effects on cell survival and neuronal differentiation. *J Neurochem* 2006;97:69–78.
- Tilson HA. Neurotoxicology risk assessment guidelines: developmental neurotoxicology. *Neurotoxicology* 2000;21(1–2):189–94.
- Woehrling EK, Hill EJ, Coleman MD. Development of a neurotoxicity test-system, using human post-mitotic, astrocytic and neuronal cell lines in co-culture. *Toxicol In Vitro* 2007;21(7):1241–6.
- Woehrling EK, Hill EJ, Coleman MD. Evaluation of the importance of astrocytes when screening for acute toxicity in neuronal cell systems. *Neurotox Res* 2010;17(2):103–13.